GEOLOGY | THE GEOLOGICAL SOCIETY OF AMERICA®

https://doi.org/10.1130/G46338.1

Manuscript received 3 April 2019
Revised manuscript received 10 July 2019
Manuscript accepted 11 August 2019

Earliest Jurassic U-Pb ages from carbonate deposits in the Navajo Sandstone, southeastern Utah, USA

Judith Totman Parrish[1]*, E. Troy Rasbury[2], Marjorie A. Chan[3] and Stephen T. Hasiotis[4]
[1]Department of Geological Sciences, University of Idaho, P.O. Box 443022, Moscow, Idaho 83844, USA
[2]Department of Geosciences, Stony Brook University, Stony Brook, New York 11794, USA
[3]Department of Geology and Geophysics, University of Utah, 115 S 1460 E, Room 383, Salt Lake City, Utah 84112-0102, USA
[4]Department of Geology, University of Kansas, 115 Lindley Hall, 1475 Jayhawk Boulevard, Lawrence, Kansas 66045-7594, USA

ABSTRACT

New uranium-lead (U-Pb) analyses of carbonate deposits in the Navajo Sandstone in southeastern Utah (USA) yielded dates of 200.5 ± 1.5 Ma (earliest Jurassic, Hettangian Age) and 195.0 ± 7.7 Ma (Early Jurassic, Sinemurian Age). These radioisotopic ages—the first reported from the Navajo erg and the oldest ages reported for this formation—are critical for understanding Colorado Plateau stratigraphy because they demonstrate that initial Navajo Sandstone deposition began just after the Triassic and that the base of the unit is strongly time-transgressive by at least 5.5 m.y.

INTRODUCTION

The Navajo Sandstone in southeastern Utah (United States) represents the largest erg in Earth history (e.g., Blakey et al., 1988), cropping out on much of the Colorado Plateau (Fig. 1). Fossils are generally lacking, poorly preserved, and/or not age diagnostic. Determining the age of the Navajo Sandstone has, therefore, been challenging. The Navajo Sandstone contains carbonate deposits laid down in lakes and springs (Parrish et al., 2017) from which we report the first radioisotopic ages, acquired by U-Pb dating. The dates reported here set the stage for future work on the development of the Navajo erg and provide a framework for understanding mechanisms of the evolution of the basin in the Jurassic Period.

PREVIOUS WORK ON THE AGE OF THE NAVAJO SANDSTONE

The Navajo Sandstone is the upper formation of the Glen Canyon Group, which in southern Utah and northern Arizona includes the Wingate Sandstone, Moenave Formation, Kayenta Formation, and Navajo Sandstone (generalized in Fig. DR1A in the GSA Data Repository[1]). These are lithostratigraphic units, and definition of the boundaries between them is commonly arbitrary, particularly where they interfinger and/or have gradational relationships. The literature on the Glen Canyon Group is voluminous, and a comprehensive review is outside the scope of this report. Useful general reviews are Blakey (2008) and Dickinson (2018), and additional reviews can be found in Peterson and Pipiringos (1979), Blakey (1989), and Sprinkel et al. (2011), as well as others.

The Wingate and Navajo Sandstones are predominately eolian (Blakey, 1989); the Moenave and Kayenta Formations contain interbedded eolian, fluvial, and lacustrine deposits (e.g., Clemmensen et al., 1989; Blakey, 2008; Suarez et al., 2017). The Moenave Formation is divided into two members, the Dinosaur Canyon Member and the overlying Whitmore Point Member. The Moenave Formation is overlain by the Springdale Sandstone, which has been assigned variously as the upper member of the Moenave Formation (Steiner, 2014a) or, more commonly, the lower member of the overlying Kayenta Formation (Lucas and Tanner, 2006; Dickinson, 2018, p. 93). In east-central Utah, the Glen Canyon Group consists solely of the Wingate Sandstone, Kayenta Formation, and Navajo Sandstone. The Kayenta Formation interfingers with the lower part of the Navajo Sandstone across a broad region from southwestern Utah to northeastern Arizona (Blakey, 1989; Hassan et al., 2018). The Glen Canyon Group is underlain by the Upper Triassic Chinle Formation, which includes the Black Ledge sandstone (e.g., Blakey, 2008; Fig. DR1A).

Age assignments of the Glen Canyon Group and underlying formations have been in a state of flux (Marsh, 2014), partly because of discrepancies between the geochronological and biostratigraphic records—a global problem in chronostratigraphy—but also because of possible overreliance on the continental biostratigraphic record (Olsen et al., 2010; see also Irmis et al., 2010; Marsh, 2014). Quantitative age estimates have come from detrital zircon (DZ) and magnetostratigraphy (Fig. 2).

The Kayenta Formation, Moenave Formation, and Black Ledge sandstone have yielded DZ ages broadly consistent with their depositional ages as determined from biostratigraphy or magnetostratigraphy (Dickinson and Gehrels, 2009a; Table DR1 in the Data Repository). Marsh (2014) dated the Kayenta Formation with DZ in northern Arizona at 183.7 ± 1.7 Ma, ~12 m.y. younger than the dates obtained by Dickinson and Gehrels (2009a) from their closest sample location of the Kayenta Formation near Moenkopi, Arizona (Fig. 1; Table DR2). DZ ages from the Moenave Formation west of Kanab, Utah, yielded dates ca. 201.3 Ma (Suarez et al., 2017; Fig. 2; Table DR2). The Chinle Formation, which underlies the Glen Canyon Group, is well dated using DZ (Irmis et al., 2011; see also Riggs et al., 2003; Ramezani et al., 2011). The youngest dates from the Chinle Formation are 203–204 Ma (Rhaetian) from the

*E-mail: jparrish@uidaho.edu

[1]GSA Data Repository item 2019359, details of methods, sample descriptions, and supplementary tables and figures, is available online at http://www.geosociety.org/datarepository/2019/, or on request from editing@geosociety.org.

CITATION: Parrish, J.T., et al., 2019, Earliest Jurassic U-Pb ages from carbonate deposits in the Navajo Sandstone, southeastern Utah, USA: Geology, v. 47, p. , https://doi.org/10.1130/G46338.1

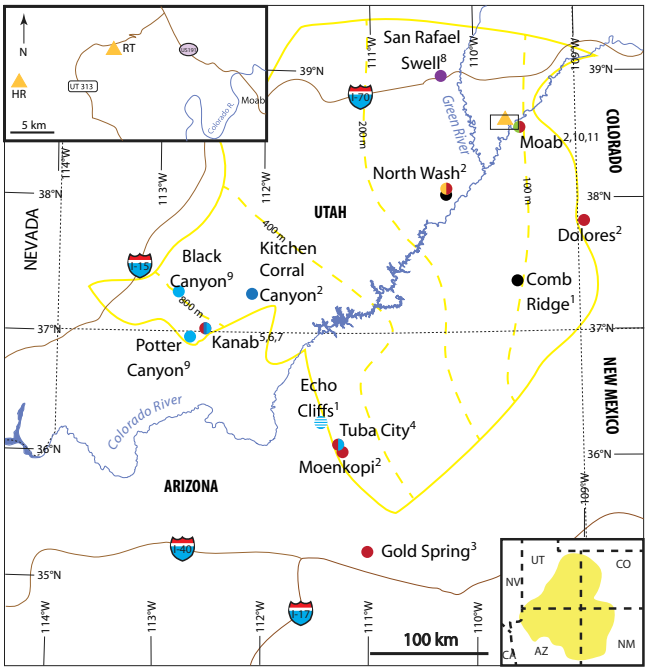

Figure 1. Map of study area and sample locations, southeastern Utah and surrounding areas (USA) (see Table DR3 [see footnote 1] for more information). Colors indicate formations sampled; see Figure 2 for color explanation. Inset at lower right shows outline of Colorado Plateau (UT—Utah; CO—Colorado; NV—Nevada; CA—California; AZ—Arizona; NM—New Mexico). Inset at upper left is location enlargement near Moab, Utah (black outline box in main map), marking sample locations for this study: Rocky Tops (RT), 38.62881°N, 109.77227°W; Horsethief Road (HR), 38.597°N, 109.88651°W. Solid yellow line shows generalized outline of Navajo Sandstone outcrop; dotted yellow lines are isopachs (Dickinson, 2018, his figure 55). Localities are from: 1—Molina-Garza et al. (2003); 2—Dickinson and Gehrels (2009a); 3—Marsh (2014); 4—Bazard and Butler (1991); 5—Steiner (2014a); 6—Steiner (2014b); 7—Steiner and Tanner (2014); 8—Umbarger (2018); 9—Suarez et al. (2017); 10—Steiner and Helsley (1974); 11—this study.

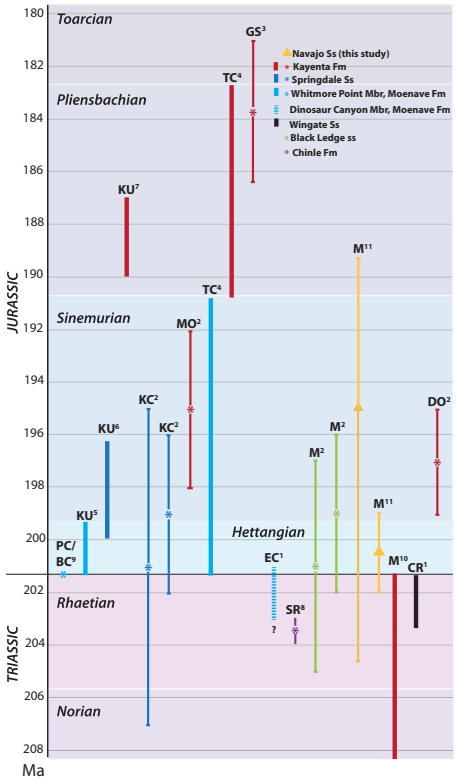

Figure 2. Summary of geochronological data on Glen Canyon Group (southwestern USA) and selected subjacent strata. Asterisks are detrital zircon (DZ) dates; triangles are U-Pb dates from this study. Thin vertical lines (error bars) on DZ dates were provided by their respective authors, except for DZ ages at Potter Canyon and Black Canyon (Suarez et al., 2017); those two ages and their error bars not resolvable at this scale. Thick vertical lines are ages specified from magnetostratigraphy as reported by their respective authors. Data are arranged roughly west (left) to east (right). PC/BC—Potter Canyon, Arizona (AZ), and Black Canyon, Utah (UT); KU—Kanab, UT, area; KC—Kitchen Corral Canyon, UT; MO—Moenkopi, AZ; TC—Tuba City area, AZ; GS—Gold Spring, AZ; EC—Echo Cliffs, AZ; SR—San Rafael Swell, UT; M—Moab, UT, area; CR—Comb Ridge, UT; DO—Dolores, Colorado. North Wash, UT (Fig. 1), is not included because DZ ages were much older than depositional ages (Dickinson and Gehrels, 2009a, 2009b; Table DR1 [see footnote 1]). Data specifics are provided in Table DR2. Time scale is from Gradstein et al. (2012); Norian-Rhaetian boundary is from Kent et al. (2017). Superscripts are citations from Figure 1 caption. Ss and ss—sandstone; Fm—formation; Mbr—member.

lower part of the Church Rock Member in the San Rafael Swell (Umbarger, 2018).

Efforts to define ages based on magnetostratigraphy of the Glen Canyon Group have also yielded age estimates. These results were calibrated against the Newark Basin (northeastern United States) magnetostratigraphy (Molina-Garza et al., 2003; Kent et al., 2017; Suarez et al., 2017), paleopole paths (Steiner and Helsley, 1974; Bazard and Butler, 1991), or the Paris Basin (France) (Steiner, 2014a, 2014b; Steiner and Tanner, 2014; Yang et al., 1996). With the exception of the estimates by Bazard and Butler (1991), these results are broadly consistent with the observed stratigraphic succession (Fig. DR1A; Table DR2). Importantly, Steiner and Tanner (2014) reported that the Kayenta Formation in the Moab, Utah, region was not correlative with the Kayenta Formation near Kanab, Utah; Steiner and Helsley (1974) placed the Kayenta Formation in the Moab area in the Late Triassic.

The Moenave Formation in the Kanab area has yielded bio-, chemo-, and magnetostratigraphic, as well as DZ, data (Donohoo-Hurley et al., 2010; Lucas et al., 2011; Suarez et al., 2017). Suarez et al. (2017) built on and corrected the magneto- and biostratigraphy of Donohoo-Hurley et al. (2010) and Lucas et al. (2011) at Potter Canyon, Utah, who placed a brief reversed polarity interval in the Whitmore Point Member in the latest Triassic. Suarez et al.'s (2017) DZ ages led them to conclude that the reversed polarity interval likely correlates to one of such intervals in the Hettangian in the Newark Basin (Kent et al., 2017).

METHODS

Samples were collected from six carbonate units described by Parrish et al. (2017) in the erg margin of the Navajo Sandstone (Fig. 1; see sample descriptions in Table DR3). They were analyzed by laser ablation for U/Pb (Table DR4); three samples were then chosen for isotope dilution analyses.

The carbonate samples were slabbed (1–2 cm long, 1–2 mm thick) and polished for laser ablation–inductively coupled plasma–mass spectrometry (LA-ICPMS). Line scans with LA-ICPMS helped identify areas of elevated U/Pb, which were subsequently targeted for spot analyses. National Institute of Standards and Technology standard NIST612 (trace elements in glass) and the carbonate standard WC-1 (Roberts et al., 2017) were used to correct for drift in U and Pb and for Pb isotope fractionation, and to correct downhole fractionation between U and Pb using Iolite software (Paton et al., 2011). Laser ablation results are provided in Table DR4.

The samples subjected to full analysis were 0805123 and 0805132 from the Rocky Tops locality (Fig. DR1B) and 0805032 from the Horsethief Road locality of Parrish et al. (2017). Samples were microsampled with a Dremel tool, spiked with a mixed ^{236}U-^{205}Pb spike, and dissolved in nitric acid. The samples were capped and left on a hotplate for >12 h before being dried for column chemistry.

The Pb and U cuts were both run on a NuII MC-ICPMS using a desolvating nebulizer in the Facility for Isotope Research and Student Training (FIRST) lab at Stony Brook University, New York, USA. The lead isotope standard reference material (SRM) 981 was used for Pb analyses, and New Brunswick Laboratory (NBL) CRM-112-a (uranium metal assay and isotopic standard) was used for U analyses. Samples were bracketed by standards, and the bracketing

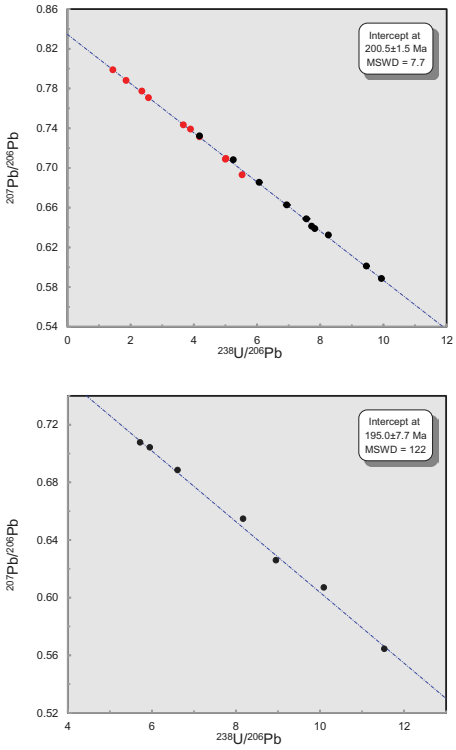

Figure 3. Three-dimensional U-Pb Tera-Wasserburg plot, projected to two dimensions, where age represents forced intersection with concordia curve (Ludwig, 2003). Error ellipses are smaller than spots and difficult to see. Two-sigma errors are shown in Table 1. A: Data from samples 0805132 (red circles) and 0805123 (black circles) from Rocky Tops locality, Utah, USA. B: Data from sample 0805032 from Horsethief Road locality, Utah. See Figure 1 for sample localities. MSWD—mean standard weighted deviation.

standards were used for fractionation correction. Data were reduced using the PBDAT program of Ludwig (1993), followed by IsoExcel (Ludwig, 2003). Data are plotted on Tera-Wasserburg plots (Fig. 3), using the total Pb-U approach, where the upper intercept is meaningless (and not reported) and the lower intercept is the age of the sample. More details on the methods are provided in the Data Repository (methods and descriptions; details of the analytical results are in Table 1 and Table DR4).

RESULTS

The sampled limestone at Rocky Tops lies 65 m above the base of the Navajo Sandstone (Fig. DR1B), and at Horsethief Road, ~90 m above the base of the Navajo Sandstone (estimated using Google Earth). The Horsethief Road site lies 11 km west-southwest of the Rocky Tops site. The base of the Navajo Sandstone is here defined as the top of the last occurrence of red sandstone with fluvial sedimentary structures.

Of the three samples that were screened from Horsethief Road, two had favorable U/Pb (Table DR4). The Horsethief Road sample analyzed by isotope dilution gave an age of 195.0 ± 7.7 Ma (Sinemurian; Fig. 2). All three of the samples from Rocky Tops had favorable U/Pb. The two samples of carbonate rocks analyzed by isotope dilution from Rocky Tops yielded overlapping ages and, combined, give an age of 200.5 ± 1.5 Ma (Hettangian). Other samples had obvious diagenetic alteration or had low U/Pb ratios and were not processed further. Sample descriptions are provided in Table DR3.

DISCUSSION AND IMPLICATIONS

Uranium-lead (U-Pb) dating of carbonates is a well-accepted geochronologic method (Rasbury and Cole, 2009), and the application of LA-ICPMS analyses has greatly improved the ability to identify samples with favorable U/Pb (Roberts et al., 2017), as shown here.

A summary of the chronostratigraphic information for the Glen Canyon Group and selected subjacent units is illustrated in Figure 2. The patterns are somewhat obscured by the data from Bazard and Butler (1991), who gave stage-level designations to their magnetostratigraphy near Tuba City, Arizona. Setting these aside, the data are, within error, consistent with the observed stratigraphic sequence from the Chinle Formation to the Kayenta Formation (Fig. DR1A). Moreover, the Kayenta Formation appears to be older in the east, becoming younger to the west and south.

Given the consistency of these data, the ages obtained here for the eastern Navajo Sandstone stand out as being too old. The Sinemurian age at Horsethief Road is slightly older than previous interpretations of the age of the lower part of the Navajo Sandstone (e.g., Blakey, 2008; Dickinson, 2018, and references therein). The Hettangian age for the Rocky Tops samples in this study, however, places the lower part of the Navajo Sandstone much older than previously suggested (e.g., Peterson and Pipiringos, 1979; Dickinson, 2018; and many others).

Given the spotty nature of quantitative data on the age of the Glen Canyon Group, a full assessment of the significance of these results must be tentative. Much of the information comes from magnetostratigraphy, which is subject to error

TABLE 1. RESULTS OF SAMPLE ANALYSIS

Sample number	Weight (mg)	U (ppm)	Pb (ppm)	$^{238}U/^{206}Pb$	2σ error (%)	$^{206}Pb/^{204}Pb$	2σ error (%)	$^{207}Pb/^{206}Pb$	2σ error (%)	$^{208}Pb/^{206}Pb$	2σ error (%)
0805032-1	8.8	3.3	0.9	10.09	0.3	26.402	0.15	0.60711	0.05	1.43223	0.06
0805032-2	13.6	1.4	0.7	5.95	0.3	22.456	0.14	0.70432	0.11	1.68984	0.12
0805032-3	8.3	2.4	0.8	8.17	0.3	24.265	0.15	0.65479	0.08	1.55516	0.09
0805032-4	16.1	3.0	1.6	5.72	0.2	22.477	0.14	0.70771	0.07	1.71176	0.08
0805032-5	8.9	2.7	1.2	6.61	0.3	23.033	0.14	0.68857	0.09	1.65204	0.10
0805032-6	17.4	2.9	0.9	8.95	0.2	25.616	0.14	0.62595	0.05	1.49467	0.05
0805032-7	18.1	4.3	0.9	11.53	0.2	28.571	0.14	0.56451	0.04	1.33547	0.04
0805123-1	22.1	2.3	1.7	4.18	0.9	21.554	0.09	0.73217	0.01	1.78462	0.01
0805123-2	18.1	5.4	1.8	8.26	0.6	25.251	0.03	0.63243	0.04	1.52201	0.03
0805123-3	33.9	4.0	0.1	5.25	0.6	22.350	0.04	0.70813	0.06	1.72084	0.05
0805123-4	31.7	5.3	1.9	7.73	0.8	24.875	0.07	0.64133	0.01	1.54701	0.02
0805123-5	17.7	6.1	2.3	7.56	1.1	24.560	0.11	0.64875	0.12	1.56531	0.04
0805123-6	22.9	3.6	1.7	6.07	1.1	23.137	0.11	0.68549	0.02	1.66131	0.01
0805123-7	23	6.1	1.7	9.46	0.70	26.693	0.05	0.60113	0.04	1.44394	0.02
0805123-8	23.1	5.4	2.2	6.94	1.14	23.970	0.12	0.66269	0.07	1.60302	0.03
0805123-9	23	6.4	1.7	9.94	0.57	27.310	0.01	0.58858	0.03	1.40842	0.02
0805123-10	23.2	5.7	2.0	7.83	0.7	24.971	0.05	0.63885	0.07	1.54119	0.04
0805132B-1	24.9	1.6	1.0	5.02	0.65	22.293	0.04	0.70951	0.07	1.72472	0.05
0805132B-2	29.5	0.5	1.1	1.86	1.1	19.925	0.11	0.78806	0.07	1.93143	0.07
0805132B-3	17.4	1.3	1.8	2.36	0.98	20.201	0.10	0.77730	0.06	1.90264	0.04
0805132B-5	19.1	0.9	0.7	2.57	0.62	20.405	0.01	0.77074	0.01	1.88945	0.01
0805132B-4	28.9	1.1	1.3	4.18	0.64	21.584	0.04	0.73138	0.01	1.78573	0.01
0805132R-1	19.5	2.7	1.4	5.53	0.70	22.868	0.04	0.69300	0.05	1.682	0.08
0805132R-2	22.2	0.8	1.8	1.44	0.60	19.637	0.02	0.79876	0.01	1.95787	0.01
0805132R-3	30	0.9	2.3	3.90	0.97	21.347	0.10	0.739051	0.02	1.80488	0.01
0805132R-4	27.7	1.8	1.5	3.67	0.62	21.202	0.03	0.7434	0.03	1.81408	0.03
0805132R-5	25.2	3.8	2.3	5.00	0.56	22.336	0.01	0.708713	0.13	1.72659	0.08

Note: Samples were spiked with a mixed $^{205}Pb/^{236}U$ spike to obtain Pb and U concentrations. Concentration errors are <0.5%. Aliquots were corrected for fractionation by standard bracketing. Total procedural blacks are <50 pg for both Pb and U. PBDAT software (Ludwig, 1993) was used for data reduction, including blank subtraction and error propagation. Samples 0805132B and 0805132R designate brown and red aliquots of this sample.

because of gaps in the rock record that can obscure the pattern of reversals. In addition, magneto- and biostratigraphic time scales are only just starting to be tied to radioisotopic dates at a level of detail that makes connecting records worldwide possible. For example, Kent et al. (2017), building on years of previous work, constructed a detailed magnetostratigraphic section for the continental (lacustrine) Newark Basin tied to biostratigraphic, radioisotopic, and astrochronologic records, allowing for study of the time scale in great detail. This record has been successfully tied to other records (e.g., Hüsing et al., 2014; Olsen et al., 2018), including the marine Paris Basin, to which Steiner (2014a, 2014b) and Steiner and Tanner (2014) compared their data (Fig. 2). On the Colorado Plateau, the time scale of Kent et al. (2017) has, to date, been compared with the Triassic record (Kent et al., 2018; Olsen et al., 2019).

The results presented here indicate that the base of the Navajo Sandstone is time-transgressive, becoming younger to the southwest. The base is time-transgressive by at least 5.5 m.y. based on the information in Figure 2 (in comparison to DZ data from near Moenkopi, Arizona; Dickinson and Gehrels, 2009a,) and perhaps as long as 20 m.y. (in comparison to DZ data at Gold Spring, Arizona; Marsh, 2014).

The lower part of the Navajo Sandstone intertongues with the Kayenta Formation (Blakey, 1989, 2008; Hassan et al., 2018). Although the Navajo erg is recognized to have eventually overstepped the Kayenta fluvial system, the timing of overstepping has been unclear (e.g., Blakey, 2008; Dickinson, 2018, p. 93). Fluvial paleocurrent indicators of the Kayenta Formation indicate a westward or northwestward flow (Blakey, 2008; Dickinson, 2018), whereas the paleowind direction indicators in the Navajo Sandstone are predominately toward the southeast (Peterson, 1988). Thus, some Kayenta sand was transported through or around the erg in rivers and then transported back to the Navajo erg by winds from the northwest (Peterson, 1988; Parrish and Peterson, 1988). How this sand transport pattern evolved through time as the Navajo Sandstone overstepped the Kayenta river system remains an open question.

The data presented here indicate that the oldest part of the Navajo erg, *per se*, is in the eastern part of the basin. However, the Navajo Sandstone may have been part of a much larger erg complex including the Nugget Sandstone to the northeast, the lower part of which has been dated biostratigraphically as Late Triassic (Britt et al., 2016). The Nugget Sandstone is lithostratigraphically correlative with the entire Glen Canyon Group, but the geochronological constraints higher in the Nugget Sandstone are poor (Sprinkel et al., 2011).

The river sediments deposited as the Kayenta Formation were pushed farther south by the encroachment of the Navajo erg from the northeast (Blakey, 1989). This erg expansion is generally interpreted as aridification of the region (e.g., Hassan et al., 2018), but this raises the question (alluded to above) on the origination of the large volume of sand that makes up the Navajo Sandstone in the west (Fig. 1). The very young date for the Kayenta Formation obtained by Marsh (2014) suggests that the Kayenta rivers may have continued to supply sand throughout deposition of the Navajo Sandstone, but given that the winds were from the northwest (Peterson, 1988), whether those or other rivers could have continued to be the source of the sand or whether there was reworking from older erg deposits is unclear.

Another implication of the ages reported in the Moab area for the uppermost Chinle Formation (Umbarger, 2018; Dickinson and Gehrels, 2009a), Kayenta Formation (Steiner and Helsley, 1974), and Navajo Sandstone (this study) is that the uppermost part of the Chinle Formation, the Wingate Sandstone, the Kayenta Formation, and the lower part of the Navajo Sandstone all were deposited within ~2–3 m.y. This would be consistent with filling of a structural trough just west of the Uncompahgre highlands (Blakey, 2008), after which additional sediment bypassed the area and was deposited farther west. Preliminary observations indicate that there may be more surfaces in the Navajo Sandstone that were exposed for longer in the Moab area than farther west (unpublished observations of authors S.T. Hasiotis, M.A. Chan, and J.T. Parrish), where sedimentation was more continuous.

Dickinson and Gehrels (2003, 2008, 2009a, 2009b) provided dates for all of the Glen Canyon Group formations, but their samples were stratigraphically unconstrained (Dickinson and Gehrels, 2009b), as many were collected from fallen blocks. This is true for several other DZ ages, the exception being those of Suarez et al. (2017). Vertical trends remain unknown. Much more work, such as that proposed by Olsen et al. (2010), is required to understand the stratigraphic and climatic implications of the ages reported here.

CONCLUSIONS

The U-Pb date of 200.5 ± 1.5 Ma in a carbonate unit in the lower part of the Navajo Sandstone near Moab, Utah, places that part of the Navajo Sandstone near the beginning of the Jurassic Period, in the Hettangian Age; an additional date of 195.0 ± 7.7 Ma (Sinemurian) is also older than previously suggested ages for the Navajo Sandstone. The Hettangian age is the oldest reported for the Navajo Sandstone and demonstrates the critical need for reevaluation of the chronostratigraphy of the Glen Canyon Group to understand its depositional history and basinal events. These dates suggest a new framework for stratigraphic, sedimentologic, and paleontologic studies across the Western Interior of the United States.

ACKNOWLEDGMENTS

We are grateful to Rebecca Hunt-Foster (formerly U.S. Bureau of Land Management Canyon Country District paleontologist) for help with permits and information. This work was funded in part by National Science Foundation (NSF) grants EAR 1349560 to Parrish, EAR 1349564 to Chan, and EAR 1349558 to Hasiotis. Rasbury acknowledges support from NSF grant EAR 1814051. Rasbury acknowledges Bridget Becchina (Ward Melville High School, Setauket East Setauket, New York, USA) and James Edmonds (Stony Brook University, New York) for help with laser ablation under the direction of FIRST lab manager Katie Wooton. Some instrumentation used for this work was funded through NSF Major Research Instrumentation grant EAR0959524.

REFERENCES CITED

Bazard, D.R., and Butler, R.F., 1991, Paleomagnetism of the Chinle and Kayenta Formations, New Mexico and Arizona: Journal of Geophysical Research, v. 96, p. 9847–9871, https://doi.org/10.1029/91JB00336.

Blakey, R.C., 1989, Triassic and Jurassic geology of the southern Colorado Plateau, *in* Jenney, J.P., and Reynolds, S.J., eds., Geologic Evolution of Arizona: Arizona Geological Society Digest 17, p. 369–396.

Blakey, R.C., 2008, Pennsylvanian–Jurassic sedimentary basins of the Colorado Plateau and southern Rocky Mountains, *in* Miall, A.D., ed., The Sedimentary Basins of the United States and Canada: Amsterdam, Elsevier B.V., Sedimentary Basins of the World, v. 5, p. 245–296, https://doi.org/10.1016/S1874-5997(08)00007-5.

Blakey, R.C., Peterson, F., and Kocurek, G., 1988, Synthesis of late Paleozoic and Mesozoic eolian deposits of the Western Interior of the United States: Sedimentary Geology, v. 56, p. 3–125, https://doi.org/10.1016/0037-0738(88)90050-4.

Britt, B.B., Chure, D.J., Engelmann, G.F., and Shumway, J.D., 2016, Rise of the erg—Paleontology and paleoenvironments of the Triassic-Jurassic transition in northeastern Utah: Geology of the Intermountain West, v. 3, p. 1–32, https://doi.org/10.31711/giw.v3i0.5.

Clemmensen, L.B., Olsen, H., and Blakey, R.C., 1989, Erg-margin deposits in the Lower Jurassic Moenave Formation and Wingate Sandstone, southern Utah: Geological Society of America Bulletin, v. 101, p. 759–773, https://doi.org/10.1130/0016-7606(1989)101<0759:EMDITL>2.3.CO;2.

Dickinson, W.R., 2018, Tectonosedimentary Relations of Pennsylvanian to Jurassic Strata on the Colorado Plateau: Geological Society of America Special Paper 533, 184 p., https://doi.org/10.1130/SPE533.

Dickinson, W.R., and Gehrels, G.E., 2003, U-Pb ages of detrital zircons from Permian and Jurassic eolian sandstones of the Colorado Plateau, USA: Paleogeographic implications: Sedimentary Geology, v. 163, p. 29–66, https://doi.org/10.1016/S0037-0738(03)00158-1.

Dickinson, W.R., and Gehrels, G.E., 2008, Sediment delivery to the Cordilleran foreland basin: Insights from U-Pb ages of detrital zircons in Upper Jurassic and Cretaceous strata of the Colorado Plateau: American Journal of Science, v. 308, p. 1041–1082.

Dickinson, W.R., and Gehrels, G.E., 2009a, Use of U-Pb ages of detrital zircons to infer maximum depositional ages of strata: A test against a Colorado Plateau Mesozoic database: Earth and Planetary Science Letters, v. 288, p. 115–125, https://doi.org/10.1016/j.epsl.2009.09.013.

Dickinson, W.R., and Gehrels, G.E., 2009b, U-Pb ages of detrital zircons in Jurassic eolian and

associated sandstones of the Colorado Plateau: Evidence for transcontinental dispersal and intraregional recycling of sediment: Geological Society of America Bulletin, v. 121, p. 408–433, https://doi.org/10.1130/B26406.1.

Donohoo-Hurley, L.L., Geissman, J.W., and Lucas, S.G., 2010, Magnetostratigraphy of the uppermost Triassic and lowermost Jurassic Moenave Formation, western United States: Correlation with strata in the United Kingdom, Morocco, Turkey, Italy, and eastern United States: Geological Society of America Bulletin, v. 122, p. 2005–2019, https://doi.org/10.1130/B30136.1.

Gradstein, F.M., Ogg, J.G., and Hilgen, F.J., 2012, On the Geologic Time Scale: Newsletters on Stratigraphy, v. 45, p. 171–188, https://doi.org/10.1127/0078-0421/2012/0020.

Hassan, M.S., Venetikidis, A., Bryant, G., and Miall, A.D., 2018, The sedimentology of an erg margin: The Kayenta–Navajo transition (Lower Jurassic), Kanab, Utah, U.S.A.: Journal of Sedimentary Research, v. 88, p. 613–640, https://doi.org/10.2110/jsr.2018.31.

Hüsing, S.K., Beniest, A., van der Boon, A., Abels, H.A., Deenen, M.H.L., Ruhl, M., and Krijgsman, W., 2014, Astronomically-calibrated magnetostratigraphy of the Lower Jurassic marine successions at St. Audrie's Bay and East Quantoxhead (Hettangian–Sinemurian; Somerset, UK): Palaeogeography, Palaeoclimatology, Palaeoecology, v. 403, p. 43–56, https://doi.org/10.1016/j.palaeo.2014.03.022.

Irmis, R.B., Martz, J.W., Parker, W.G., and Nesbitt, S.J., 2010, Re-evaluating the correlation between Late Triassic terrestrial vertebrate biostratigraphy and the GSSP-defined marine stages: Albertiana, v. 38, p. 40–52.

Irmis, R.B., Mundil, R., Martz, J.W., and Parker, W.G., 2011, High-resolution U-Pb ages from the Upper Triassic Chinle Formation (New Mexico, USA) support a diachronous rise of dinosaurs: Earth and Planetary Science Letters, v. 309, p. 258–267, https://doi.org/10.1016/j.epsl.2011.07.015.

Kent, D.V., Olsen, P.E., and Muttoni, G., 2017, Astrochronostratigraphic polarity time scale (APTS) for the Late Triassic and Early Jurassic from continental sediments and correlation with standard marine stages: Earth-Science Reviews, v. 166, p. 153–180, https://doi.org/10.1016/j.earscirev.2016.12.014.

Kent, D.V., et al., 2018, Empirical evidence for stability of the 405-kiloyear Jupiter–Venus eccentricity cycle over hundreds of millions of years: Proceedings of the National Academy of Sciences of the United States of America, v. 115, p. 6153–6158, https://doi.org/10.1073/pnas.1800891115.

Lucas, S.G., and Tanner, L.H., 2006, The Springdale Member of the Kayenta Formation, Lower Jurassic of Utah-Arizona, *in* Harris, J.D., et al., eds., The Triassic-Jurassic Terrestrial Transition: New Mexico Museum of Natural History and Science Bulletin 37, p. 71–76.

Lucas, S.G., Tanner, L.H., Donohoo-Hurley, L.L., Geissman, J.W., Kozur, H.W., and Weems, R.E., 2011, Position of the Triassic-Jurassic boundary and timing of the end-Triassic extinctions on land: Data from the Moenave Formation on the southern Colorado Plateau, USA: Palaeogeography, Palaeoclimatology, Palaeoecology, v. 302, p. 194–205, https://doi.org/10.1016/j.palaeo.2011.01.009.

Ludwig, K.R., 1993, PBDAT: A computer program for processing Pb-U-Th isotope data, version 1.2: U.S. Geological Survey Open-File Report 88-542, 33 p., https://doi.org/10.3133/ofr88542.

Ludwig, K.R., 2003, User's manual for Isoplot 3.00: A geochronological toolkit for Microsoft Excel: Berkeley Geochronology Center Special Publication 4, 70 p.

Marsh, A.D., 2014, Preliminary U-Pb detrital zircon dates from the Kayenta Formation of Arizona: PaleoBios, v. 32, no. 1, Suppl. (Western Association of Vertebrate Paleontology Annual Meeting, Program with Abstracts), p. 10.

Molina-Garza, R.S., Geissman, J.W., and Lucas, S.G., 2003, Paleomagnetism and magnetostratigraphy of the lower Glen Canyon and upper Chinle Groups, Jurassic-Triassic of northern Arizona and northeast Utah: Journal of Geophysical Research, v. 108, 2181, https://doi.org/10.1029/2002JB001909.

Olsen, P.E., et al., 2010, The Colorado Plateau Coring Project (CPCP): 100 million years of Earth system history: Earth Science Frontiers, v. 17, p. 55–63.

Olsen, P.E., et al., 2018, Colorado Plateau Coring Project, Phase I (CPCP-I): A continuously cored, globally exportable chronology of Triassic continental environmental change from western North America: Scientific Drilling, v. 24, p. 15–40, https://doi.org/10.5194/sd-24-15-2018.

Olsen, P.E., Laskar, J., Kent, D.V., Kinney, S.T., Reynolds, D.J., Sha, J.G., and Whiteside, J.H., 2019, Mapping solar system chaos with the Geological Orrery: Proceedings of the National Academy of Sciences of the United States of America, v. 116, p. 10664–10673, https://doi.org/10.1073.pnas.1813901116.

Parrish, J.T., and Peterson, F., 1988, Wind directions predicted from global circulation models and wind directions determined from eolian sandstones of the western United States—A comparison: Sedimentary Geology, v. 56, p. 261–282, https://doi.org/10.1016/0037-0738(88)90056-5.

Parrish, J.T., Hasiotis, S.T., and Chan, M.A., 2017, Carbonate deposits in the Lower Jurassic Navajo Sandstone, southern Utah and northern Arizona: Journal of Sedimentary Research, v. 87, p. 740–762, https://doi.org/10.2110/jsr.2017.42.

Paton, C., Hellstrom, J., Paul, B., Woodhead, J., and Hergt, J., 2011, Iolite: Freeware for the visualisation and processing of mass spectrometric data: Journal of Analytical Atomic Spectrometry, v. 26, p. 2508–2518, https://doi.org/10.1039/c1ja10172b.

Peterson, F., 1988, Pennsylvanian to Jurassic eolian transportation systems in the western United States: Sedimentary Geology, v. 56, p. 207–260, https://doi.org/10.1016/0037-0738(88)90055-3.

Peterson, F., and Pipiringos, G.N., 1979, Stratigraphic relations of the Navajo Sandstone to Middle Jurassic formations, southern Utah and northern Arizona: U.S. Geological Survey Professional Paper 1035-B, 43 p., https://doi.org/10.3133/pp1035B.

Ramezani, J., Hoke, G.D., Fastovsky, D.E., Bowring, S.A., Therrien, F., Dworkin, S.I., Atchley, S.C., and Nordt, L.C., 2011, High-precision U-Pb zircon geochronology of the Late Triassic Chinle Formation, Petrified Forest National Park (Arizona, USA): Temporal constraints on the early evolution of dinosaurs: Geological Society of America Bulletin, v. 123, p. 2142–2159, https://doi.org/10.1130/B30433.1.

Rasbury, E.T., and Cole, J.M., 2009, Directly dating geologic events: U-Pb dating of carbonates: Reviews of Geophysics, v. 47, p. 545–548.

Riggs, N.R., Ash, S.R., Barth, A.P., Gehrels, G.E., and Wooden, J.L., 2003, Isotopic age of the Black Forest Bed, Petrified Forest Member, Chinle Formation, Arizona: An example of dating a continental sandstone: Geological Society of America Bulletin, v. 115, p. 1315–1323, https://doi.org/10.1130/B25254.1.

Roberts, N.M.W., Rasbury, E.T., Parrish, R.R., Horstwood, M.S.A., Condon, D.J., and Smith, C.J., 2017, A calcite reference material for LA-ICP-MS U-Pb geochronology: Geochemistry Geophysics Geosystems, v. 18, p. 2807–2814, https://doi.org/10.1002/2016GC006784.

Sprinkel, D.A., Kowallis, B.J., and Jensen, P.H., 2011, Correlation and age of the Nugget Sandstone and Glen Canyon Group, Utah, *in* Sprinkel, D.A., et al., eds., Sevier Thrust Belt: Northern and Central Utah and Adjacent Areas: Utah Geological Association Publication 40, p. 131–149.

Steiner, M., 2014a, Age of Lower Jurassic Springdale Sandstone of southwestern Utah from its magnetic polarity sequence: Volumina Jurassica, v. 12, no. 2, p. 23–30.

Steiner, M., 2014b, New magnetostratigraphy and paleopole from the Whitmore Point Member of the Moenave Formation at Kanab, Utah: Volumina Jurassica, v. 12, no. 2, p. 13–22.

Steiner, M.B., and Helsley, C.E., 1974, Magnetic polarity sequence of the Upper Triassic Kayenta Formation: Geology, v. 2, p. 191–194, https://doi.org/10.1130/0091-7613(1974)2<191:MPSOTU>2.0.CO;2.

Steiner, M., and Tanner, L.H., 2014, Magnetostratigraphy and paleopoles of the Kayenta Formation and the Tenney Canyon Tongue: Volumina Jurassica, v. 12, no. 2, p. 31–38.

Suarez, C.A., Knobbe, T.K., Crowley, J.L., Kirkland, J.I., and Milner, A.R.C., 2017, A chronostratigraphy assessment of the Moenave Formation, USA using C-isotope chemostratigraphy and detrital zircon geochronology: Implications for the terrestrial end Triassic extinction: Earth and Planetary Science Letters, v. 475, p. 83–93, https://doi.org/10.1016/j.epsl.2017.07.028.

Umbarger, K.F., 2018, Late Triassic North American paleodrainage networks and sediment dispersal of the Chinle Formation: A quantitative approach utilizing detrital zircons [M.S. thesis]: Lawrence, University of Kansas, 130 p.

Yang, Z., Moreau, M.-G., Bucher, H., Dommergues, J.-L., and Trouiller, A., 1996, Hettangian and Sinemurian magnetostratigraphy from Paris Basin: Journal of Geophysical Research, v. 101, p. 8025–8042, https://doi.org/10.1029/95JB03717.

Printed in USA